Hindawi Publishing Corporation
Advances in High Energy Physics
Volume 2015, Article ID 509847, 16 pages
http://dx.doi.org/10.1155/2015/509847

Research Article

Two Higgs Bosons near 125 GeV in the Complex NMSSM and the LHC Run I Data

Stefano Moretti[1] and Shoaib Munir[2]

[1]*School of Physics & Astronomy, University of Southampton, Southampton SO17 1BJ, UK*
[2]*Asia Pacific Center for Theoretical Physics, San 31, Hyoja-dong, Nam-gu, Pohang 790-784, Republic of Korea*

Correspondence should be addressed to Shoaib Munir; s.munir@apctp.org

Received 24 April 2015; Revised 14 July 2015; Accepted 30 July 2015

Academic Editor: Mark D. Goodsell

We analyse the impact of explicit CP-violation in the Higgs sector of the Next-to-Minimal Supersymmetric Standard Model (NMSSM) on its consistency with the Higgs boson data from the Large Hadron Collider (LHC). Through detailed scans of the parameter space of the complex NMSSM for certain fixed values of one of its CP-violating (CPV) phases, we obtain a large number of points corresponding to five phenomenologically relevant scenarios containing ~125 GeV Higgs boson(s). We focus, in particular, on the scenarios where the visible peaks in the experimental samples can actually be explained by two nearly mass-degenerate neutral Higgs boson states. We find that some points corresponding to these scenarios give an overall slightly improved fit to the data, more so for nonzero values of the CPV phase, compared to the scenarios containing a single Higgs boson near 125 GeV.

1. Introduction

The Higgs sector of the NMSSM [1–4] (see, e.g., [5, 6] for reviews) contains two additional neutral mass eigenstates besides the three of the Minimal Supersymmetric Standard Model (MSSM). This is due to the presence of a Higgs singlet superfield besides the two doublet superfields of the MSSM. When all the parameters in the Higgs and sfermion sectors of the NMSSM are real, one of these new Higgs states is a scalar and the other a pseudoscalar. Hence, in total three scalars, $H_{1,2,3}$, and two pseudoscalars, $A_{1,2}$, make up the neutral Higgs boson content of the model. This extended Higgs sector of the NMSSM boasts some unique phenomenological possibilities, which are either precluded or experimentally ruled out in the MSSM. For example, in the NMSSM either of the two lightest CP-even Higgs bosons, H_1 or H_2, can play the role of the ~125 GeV Standard Model- (SM-) like Higgs boson, $H_{\rm obs}$, observed at the LHC [7–9].

Of particular interest in the NMSSM is the possibility that the SM-like Higgs boson can obtain a large tree-level mass in a *natural* way, that is, without requiring large radiative corrections from the supersymmetric sectors. This happens in a specific region of the parameter space, which we refer to as the natural NMSSM, where there is a significant singlet-doublet mixing and $H_{\rm obs}$ is typically H_2. This scenario was used to explain [10–12] the enhancement in $H_{\rm obs} \to \gamma\gamma$ channel in the early LHC data. However, when the singlet-doublet mixing is too large, the properties of H_2 can deviate appreciably from an exact SM-like behaviour, resulting in a reduction of its fermionic partial decay widths. An alternative possibility in a very similar parameter space region is that of both H_1 and H_2 simultaneously having masses near 125 GeV [13–16]. In that case, the observed excess at the LHC could actually be due to a superposition of these two states, when their individual signal peaks cannot be resolved separately. One of these two Higgs bosons, typically H_1, is the singlet-like neutral state. Moreover, in [17] it was noted that the lighter one of the two pseudoscalars, A_1, when it is singlet-like, could also be nearly mass-degenerate with a SM-like H_1 near 125 GeV, instead of or even along with H_2. However, such a pseudoscalar can only contribute visibly to the measured signal strength near 125 GeV if it is produced in association with $b\bar{b}$ pair.

One of the most important yet unresolved issues in particle physics is that of the observed matter-antimatter

asymmetry in the universe. A plausible explanation for this asymmetry is electroweak (EW) baryogenesis [18, 19]. The necessary conditions for successful EW baryogenesis include the following [20]: (1) baryon number violation, (2) CP-violation, and (3) departure from equilibrium at the critical temperature of the EW symmetry breaking (EWSB) phase transition, implying that it is strongly first order. In the SM, a strongly first order EW phase transition is not possible given the measured mass of the Higgs boson at the LHC. Besides, the only source of CP-violation in the SM, the Cabibbo-Kobayashi-Maskawa matrix, is insufficient. Therefore, beyond the SM, a variety of sources of CP-violation have been proposed in the literature (for a review, see [21] and references therein). In the context of supersymmetry (SUSY), a strongly first order phase transition is possible in the MSSM only if the lightest stop has a mass below that of the top quark. This possibility has now been ruled out by SUSY searches at the LHC [22–24]. Also, the MSSM Higgs sector does not violate CP at the tree level but does so only at higher orders [25–32]. The CPV phases, transmitted radiatively to the Higgs sector via couplings to the sfermions, are tightly constrained by the measurements of fermion electric dipole moments (EDMs) [33–35]. However, these EDM constraints can be relaxed under certain conditions [27, 28, 36–41].

The NMSSM has been shown to accommodate a strongly first order EW phase transition without a light stop [42–47]. Additionally, in this model, CP-violation can be invoked explicitly in the Higgs sector even at the tree level by assuming the Higgs self-couplings, λ and κ, to be complex. Beyond the Born approximation, the phase of the SUSY-breaking Higgs-sfermion-sfermion couplings, $A_{\tilde{f}}$, where f denotes a SM fermion, is also induced in the Higgs sector, as in the MSSM. In the presence of the associated complex phases, the five neutral Higgs bosons are CP-indefinite states, due to the mixing between the scalar and pseudoscalar interaction eigenstates. CPV phases can therefore influence the phenomenology of the NMSSM Higgs bosons by, for example, modifying their mass spectrum as well as their production and decay rates [48], similarly to the MSSM [49–59]. The impact of these phases in the complex NMSSM (cNMSSM), that is, the CPV NMSSM, on the necessary conditions for successful EW phase transition was also studied some time ago [60]. The consistency of scenarios yielding the correct baryon asymmetry with the LHC Higgs boson data still remains to be studied in depth though. However, even leaving aside these considerations, the possibly distinct phenomenological scenarios that the cNMSSM can yield make it a particularly interesting model for exploration at the Run II of the LHC.

The cNMSSM has therefore been the subject of several studies recently and, in particular, some important theoretical developments have been made in the model. The dominant 1-loop corrections to the neutral Higgs sector from the (s)quark and gauge sectors were studied in [61–64], in the renormalisation group equations-improved effective potential approach. The corrections from the gaugino sector were included in [65] and, more inclusively, recently in [66]. In the Feynman diagrammatic approach, the complete 1-loop Higgs mass matrix was derived in [67] and $\mathcal{O}(\alpha_t\alpha_s)$ contributions to it were calculated in [68]. As far as the phenomenology of the Higgs bosons in the cNMSSM is concerned, the consistency of several CPV scenarios with the early results on $H_{\rm obs}$ from the LHC data was studied in detail in [48, 67]. Another distinct phenomenological scenario, possible only for nonzero CPV phases, has also been studied in [65].

The CMS and ATLAS collaborations have recently updated their measurements of $H_{\rm obs}$ signal rates in $\tau^+\tau^-$ and $b\bar{b}$ channels [69, 70]. The fact that these rates also tend to favour a SM-like $H_{\rm obs}$ is increasingly jeopardising the above-mentioned natural NMSSM scenario with large singlet-doublet mixing but only with one Higgs boson, either H_1 or H_2, around 125 GeV. This makes the scenario with both H_1 and H_2 contributing to the observed ~125 GeV signal all the more important, since it may potentially satisfy better the current Higgs boson data while still leaving plenty of room for new physics. In case of the cNMSSM, since the five neutral Higgs bosons are CP-mixed states, the scenario with mass-degenerate H_1 and H_2 can entail both the corresponding possibilities in the real NMSSM (rNMSSM), that is, mass-degenerate H_1, H_2 or $H_1/H_2, A_1$.

In this study we therefore analyse and compare the prospects for scenarios with two mass-degenerate Higgs bosons against those with a single Higgs boson near 125 GeV in the Z_3-invariant cNMSSM. We perform scans of the relevant parameter space [13] of the model using the public program NMSSMCALC [71] to search for all possible ~125 GeV Higgs boson scenarios, with the CPV phase of the coupling κ set to five different values, including 0°, the rNMSSM limit, in each case. The condition for mass-degeneracy between two Higgs bosons is imposed by requiring them to lie within 2.5 GeV of each other, which is consistent with the current mass resolution of the LHC [72], taking into account the uncertainties in the theoretical mass prediction. We then use fits to the Higgs boson data from the LHC Run I, both with $\sqrt{s} = 7$ TeV and $\sqrt{s} = 8$ TeV, as well as the Tevatron, performed using the program HiggsSignals [73], as the sole criterion for comparing the present likelihood of each of these scenarios. We also discuss how these mass-degenerate Higgs bosons can be identified at the LHC based on the signal rate double ratios introduced in [74].

The paper is organised as follows. In the next section we will briefly revisit the Higgs sector of the cNMSSM. In Section 3 we will provide details of our numerical scans and our procedure for fitting the model predictions for the Higgs boson(s) to the LHC data. In Section 4 we will discuss the results of our analysis and in Section 5 we will present our conclusions.

2. The Higgs Sector of the cNMSSM

The NMSSM contains a singlet Higgs superfield, $\widehat{S}$, besides the two $SU(2)_L$ doublet superfields,

$$\widehat{H}_u = \begin{pmatrix} \widehat{H}_u^+ \\ \widehat{H}_u^0 \end{pmatrix}, \qquad \widehat{H}_d = \begin{pmatrix} \widehat{H}_d^0 \\ \widehat{H}_d^- \end{pmatrix}, \tag{1}$$

of the MSSM. The superpotential of the NMSSM is written as

$$W_{\text{NMSSM}} = \text{MSSM Yukawa terms} + \lambda \widehat{S} \widehat{H}_u \widehat{H}_d + \frac{\kappa}{3} \widehat{S}^3, \quad (2)$$

where λ and κ are dimensionless Yukawa couplings. This superpotential is scale invariant, since the term $\mu \widehat{H}_u \widehat{H}_d$ appearing in the MSSM superpotential has been removed by imposing a discrete Z_3 symmetry. In this model, an effective μ-term, $\mu_{\text{eff}} = \lambda s$, is instead generated when the singlet field acquires a vacuum expectation value (VEV), s, which is naturally of the order of the SUSY-breaking scale.

The tree-level Higgs potential of the NMSSM, obtained from the superpotential in (2), is written in terms of the neutral scalar components of the Higgs superfields, H_u, H_d, and S, as

$$\begin{aligned} V_0 = & \left| \lambda \left(H_u^+ H_d^- - H_u^0 H_d^0 \right) + \kappa S^2 \right|^2 \\ & + \left(m_{H_u}^2 + |\lambda S|^2 \right) \left(\left| H_u^0 \right|^2 + \left| H_u^+ \right|^2 \right) \\ & + \left(m_{H_d}^2 + |\lambda S|^2 \right) \left(\left| H_d^0 \right|^2 + \left| H_d^- \right|^2 \right) \\ & + \frac{g^2}{4} \left(\left| H_u^0 \right|^2 + \left| H_u^+ \right|^2 - \left| H_d^0 \right|^2 - \left| H_d^- \right|^2 \right)^2 \\ & + \frac{g_2^2}{2} \left| H_u^+ H_d^{0*} + H_u^0 H_d^{-*} \right|^2 + m_S^2 |S|^2 \\ & + \left(\lambda A_\lambda \left(H_u^+ H_d^- - H_u^0 H_d^0 \right) S + \frac{1}{3} \kappa A_\kappa S^3 + \text{h.c.} \right), \end{aligned} \quad (3)$$

where $g^2 \equiv (g_1^2 + g_2^2)/2$, with g_1 and g_2 being the $U(1)_Y$ and $SU(2)_L$ gauge couplings, respectively, and A_λ and A_κ are the soft SUSY-breaking Higgs trilinear couplings. The scalar fields H_u, H_d, and S are developed around their respective VEVs, v_u, v_d, and s, as

$$\begin{aligned} H_d^0 &= \begin{pmatrix} \frac{1}{\sqrt{2}} \left(v_d + H_{dR} + i H_{dI} \right) \\ H_d^- \end{pmatrix}, \\ H_u^0 &= e^{i\theta} \begin{pmatrix} H_u^+ \\ \frac{1}{\sqrt{2}} \left(v_u + H_{uR} + i H_{uI} \right) \end{pmatrix}, \\ S &= \frac{e^{i\varphi}}{\sqrt{2}} \left(s + S_R + i S_I \right). \end{aligned} \quad (4)$$

The Higgs coupling parameters appearing in the potential in (3) can very well be complex, implying $\lambda \equiv |\lambda| e^{i\phi_\lambda}$, $\kappa \equiv |\kappa| e^{i\phi_\kappa}$, $A_\lambda \equiv |A_\lambda| e^{i\phi_{A_\lambda}}$, and $A_\kappa \equiv |A_\kappa| e^{i\phi_{A_\kappa}}$. As a result, V_0, evaluated at the vacuum, contains the phase combinations

$$\begin{aligned} \phi_\lambda' &\equiv \phi_\lambda + \theta + \varphi, \\ \phi_\kappa' &\equiv \phi_\kappa + 3\varphi, \\ & \phi_\lambda' + \phi_{A_\lambda}, \\ & \phi_\kappa' + \phi_{A_\kappa}. \end{aligned} \quad (5)$$

For correct EWSB, the Higgs potential should have a minimum at nonvanishing v_u, v_d, and s, which is ensured by requiring

$$\left\langle \frac{\delta V_0}{\delta \Phi} \right\rangle = 0 \quad \text{for } \Phi = H_{dR}, H_{uR}, S_R, H_{dI}, H_{uI}, S_I. \quad (6)$$

Through the above minimisation conditions the phase combinations $\phi_\lambda' + \phi_{A_\lambda}$ and $\phi_\kappa' + \phi_{A_\kappa}$ can be determined up to a twofold ambiguity by $\phi_\lambda' - \phi_\kappa'$. Thus, $\phi_\lambda' - \phi_\kappa'$ is the only physical CP phase appearing in the NMSSM Higgs sector at the tree level. Also, using these conditions, the soft mass parameters $m_{H_u}^2$, $m_{H_d}^2$, and m_S^2 can be traded for the corresponding Higgs field VEVs.

The neutral Higgs mass matrix is obtained by taking the second derivative of V_0 evaluated at the vacuum. This 5×5 matrix, $\mathscr{M}_0^2$, in the $\mathbf{H}^T = (H_{dR}, H_{uR}, S_R, H_I, S_I)$ basis, from which the massless Nambu-Goldstone mode has been rotated away, can be diagonalised using an orthogonal matrix, O, as $O^T \mathscr{M}_0^2 O = \text{diag} \left(m_{H_1}^2 \;\; m_{H_2}^2 \;\; m_{H_3}^2 \;\; m_{H_4}^2 \;\; m_{H_5}^2 \right)$. This yields the physical tree-level masses corresponding to the five mass eigenstates:

$$\left(H_1, H_2, H_3, H_4, H_5 \right)_a^T = O_{ai} \left(H_{dR}, H_{uR}, S_R, H_I, S_I \right)_i^T, \quad (7)$$

such that $m_{H_1}^2 \leq m_{H_2}^2 \leq m_{H_3}^2 \leq m_{H_4}^2 \leq m_{H_5}^2$. The elements, O_{ai}, of the mixing matrix then govern the couplings of the Higgs bosons to all the particles in the model.

The tree-level Higgs mass matrix is subject to higher order corrections from the SM fermions, from the gauge and chargino/neutralino sectors and the Higgs sector itself, as well as the sfermion sector, in case of which they are dominated by the stop contributions. Upon the inclusion of these corrections, $\Delta \mathscr{M}^2$, the Higgs mass matrix gets modified, so that

$$\mathscr{M}_H^2 = \mathscr{M}_0^2 + \Delta \mathscr{M}^2. \quad (8)$$

Explicit expressions for $\mathscr{M}_0^2$ as well as $\Delta \mathscr{M}^2$ can be found in [65–67]. Thus, beyond the Born approximation, the CPV phases of the gaugino mass parameters, $M_{1,2}$, and of $A_{\tilde{f}}$ are also radiatively induced in the Higgs sector of the NMSSM.

Therefore, when studying the phenomenology of the Higgs bosons, one needs to take into account also the parameters from the other sectors of the model. However, the most general NMSSM contains more than 130 parameters at the EW scale. Assuming the matrices for the sfermion masses and for the trilinear scalar couplings to be diagonal considerably reduces the number of free parameters. One can further exploit the fact, mentioned above, that the corrections to the Higgs boson masses from the sfermions are largely dominated by the stop sector. For our numerical analysis in the following sections, we will thus impose the following

supergravity-inspired universality conditions on the model parameters at the EW scale:

$$M_0 \equiv M_{Q_{1,2,3}} = M_{U_{1,2,3}} = M_{D_{1,2,3}} = M_{L_{1,2,3}} = M_{E_{1,2,3}},$$
$$M_{1/2} \equiv 2M_1 = M_2 = \frac{1}{3}M_3, \quad (9)$$
$$A_0 \equiv A_{\tilde{t}} = A_{\tilde{b}} = A_{\tilde{\tau}},$$

where $M^2_{Q_{1,2,3}}$, $M^2_{U_{1,2,3}}$, $M^2_{D_{1,2,3}}$, $M^2_{L_{1,2,3}}$, and $M^2_{E_{1,2,3}}$ are the squared soft masses of the sfermions, $M_{1,2,3}$ those of the gauginos, and $A_{\tilde{t},\tilde{b},\tilde{\tau}}$ the soft trilinear couplings. Altogether, the input parameters of the cNMSSM then include M_0, $|M_{1/2}|$, $|A_0|$, $\tan\beta(\equiv v_u/v_d)$, $|\lambda|$, $|\kappa|$, μ_{eff}, $|A_\lambda|$, $|A_\kappa|$, $\theta_{1/2}$, $\theta_{\tilde{f}}$, ϕ'_λ, and ϕ'_κ, where $\theta_{1/2}$ and $\theta_{\tilde{f}}$ are the phases of the unified parameters $M_{1/2}$ and A_0, respectively.

3. Numerical Analysis

As noted in the Introduction, nonzero CPV phases can modify appreciably the masses and decay widths of the neutral Higgs bosons compared to the CP-conserving case for a given set of the remaining free parameters. In the case of H_{obs} candidate in the model, whether H_1 or H_2 or even H_3, the CPV phases are thus strongly constrained by the LHC mass and signal rate measurements. This was analysed in detail in [48], where the scenarios with mass-degenerate Higgs bosons were, however, not taken into account. In the present study we thus test whether the said modifications in the Higgs boson properties with nonzero values of the phase ϕ'_κ (by which we imply ϕ_κ, which is the actual physically meaningful phase, since φ can be absorbed into ϕ'_κ by a field redefinition) can lead to a relatively improved consistency with the experimental data.

The reason for choosing ϕ'_κ as the only variable phase while setting $\theta_{1/2}$, $\theta_{\tilde{f}}$, and ϕ'_λ to 0° is that it is virtually unconstrained by the measurements of fermionic EDMs [63, 64, 67]. Furthermore, our aim here is to analyse the scenarios with a generic CPV phase and compare them with the rNMSSM limit rather than measure the effect of any of the individual phases. Note however that since only the difference $\phi'_\lambda - \phi'_\kappa$ enters the Higgs mass matrix at the tree level, the impact of a variation in ϕ'_λ is also quantified by that due to the variation in ϕ'_κ at this level. At higher orders though, a variation in ϕ'_λ has an impact on the sfermion and neutralino/chargino sectors which is independent of ϕ'_κ.

In our numerical analysis, we used the program NMSSMCALC-v1.03 [71] for computing the Higgs boson mass spectrum and decay branching ratios (BRs) for a given model input point. The public distribution of NMSSMCALC contains two separate packages, one for the rNMSSM only and the other for the cNMSSM. Some supersymmetric corrections to the Higgs boson decay widths are currently only available in the rNMSSM and hence are not included in the cNMSSM package. For consistency among our rNMSSM and cNMSSM results, we therefore set $\phi_\kappa = 0°$ in the cNMSSM package for the rNMSSM case instead of using the dedicated rNMSSM package. Furthermore, using the cNMSSM code also for the rNMSSM limit makes it convenient to draw a one-on-one correspondence between $\phi_\kappa = 0°$ case and each of $\phi_\kappa > 0°$ cases in a given scenario. This is because in the cNMSSM package, even in the rNMSSM limit, the five neutral Higgs bosons are ordered by their masses and not separated on the basis of their CP-identities. Thus, the scenario with mass-degenerate H_1, H_2, which we will henceforth refer to as the $H_{\text{obs}} = H_1 + H_2$ scenario, takes into account both the ~125 GeV H_1, H_2 and the ~125 GeV H_1, A_1 solutions of the rNMSSM without distinguishing between them. If one, conversely, uses the rNMSSM package, these two scenarios ought to be considered separately. The same is true also for the $H_{\text{obs}} = H_2 + H_3$ scenario, wherein H_2, H_3 are mass-degenerate.

The program NMSSMCALC allows one the option to include only the complete 1-loop contributions in the Higgs mass matrix or to add also the 2-loop $\mathcal{O}(\alpha_t\alpha_s)$ corrections to it. In our analysis, for a better theoretical precision, we evaluated the Higgs boson masses at the 2-loop level. In the NMSSMCALC input, one also needs to choose between the modified dimensional regularisation ($\overline{\text{DR}}$) and on-shell renormalisation schemes for calculating contributions from the top/stop sector in the program. We opted for the $\overline{\text{DR}}$ scheme for each scenario. Note though that further inclusion of $\mathcal{O}(\alpha_b\alpha_s)$, $\mathcal{O}(\alpha_t + \alpha_b + \alpha_\tau)^2$, and the recently calculated NMSSM-specific $\mathcal{O}(\alpha_\lambda + \alpha_\kappa)^2$ 2-loop corrections [75] in NMSSMCALC may have a nonnegligible impact on the Higgs boson masses and observables [76]. We, however, maintain that such contributions will only result in a slight shifting of the parameter configurations yielding solutions of our interest here, but our overall results and conclusions should still remain valid.

We performed six sets of scans of the cNMSSM parameter space by linking NMSSMCALC with the MultiNest-v2.18 [77–79] package. MultiNest performs a multimodal sampling of a theoretical model's parameter space based on Bayesian evidence estimation. However, we use this package not for drawing Bayesian inferences about the various NMSSM scenarios considered but simply to avoid a completely random sampling of the 9-dimensional model parameter space. In the program, we therefore defined a Gaussian likelihood function for H_{obs} in a given scan, assuming the experimental measurement of its mass to be 125 GeV and allowing up to ±2 GeV error in its model prediction. We set the enlargement factor reduction parameter to 0.3 and the evidence tolerance factor to a rather small value of 0.2, so that while the package was sampled more concentratedly near the central mass value, a sufficiently large number of points were collected before the scan converged. In each of the first two sets of scans we required H_1 to be H_{obs}. In the third set we imposed this requirement of consistency with H_{obs} mass on H_2, in the fourth set on H_3, in the fifth set on both H_1 and H_2, and in the sixth set on both H_2 and H_3. Each of the six sets further contained five separate scans corresponding to $\phi_\kappa = 0°$, 3°, 10°, 30°, and 60°.

The scanned ranges of the nine free parameters (after fixing the phases) of the natural NMSSM, which are uniform across all its five scenarios considered, are given in Table 1(a). Only large values of λ and κ are used in this model (with the upper cut-off on them imposed to avoid the Landau pole).

Table 1: Ranges of the NMSSM parameters scanned, with fixed ϕ_κ, for (a) each $H_{\rm obs}$ scenario in the natural NMSSM and (b) the low-λ-NMSSM scenario.

(a)

Parameter	Natural NMSSM range
M_0 (GeV)	200–2000
$M_{1/2}$ (GeV)	100–1000
A_0 (GeV)	−3000–0
$\tan\beta$	1–8
λ	0.4–0.7
κ	0.3–0.6
$\mu_{\rm eff}$ (GeV)	100–300
A_λ (GeV)	−1000–1000
A_κ (GeV)	−1000–1000

(b)

Parameter	Low-λ-NMSSM range
M_0 (GeV)	200–4000
$M_{1/2}$ (GeV)	100–2000
A_0 (GeV)	−7000–0
$\tan\beta$	5–45
λ	0.001–0.4
κ	0.001–0.3
$\mu_{\rm eff}$ (GeV)	100–2000
A_λ (GeV)	−1000–4000
A_κ (GeV)	−4000–1000

Since large radiative corrections from SUSY sectors are not necessary in the natural limit of the NMSSM, the parameters M_0, $M_{1/2}$, and A_0 are not required to take too large values. Note that while A_0 can in principle be both positive and negative, with a slightly different impact on the physical mass of the SM-like Higgs boson for an identical set of other input parameters in each case, we restricted the scans to its negative values only, in order to increase the scanning efficiency.

In the remaining sixth scan, we considered the complementary parameter space of the NMSSM, with λ and κ kept to relatively smaller (and $\tan\beta$ to larger) values, so as to prevent too large singlet-doublet mixing. In fact, for $\lambda, \kappa \to 0$, when the singlet sector gets effectively decoupled, H_1, which is by default identified with $H_{\rm obs}$, has properties very identical to the lightest Higgs boson of the MSSM. Since H_1 in such a case does not obtain a maximal tree-level mass that is possible in the most general model, large radiative corrections are needed from the SUSY sector. Hence we used slightly extended ranges of the remaining parameters, which are given in Table 1(b). This scenario, which we refer to as the low-λ-NMSSM scenario henceforth, has been included in our analysis in order to compare the inferences made for the natural NMSSM with an approximate MSSM limit of the model.

Once the scans had been completed, we filtered the points obtained with each by further imposing $123\ {\rm GeV} \leq m_{H_{\rm obs}} \leq 127\ {\rm GeV}$. Note that, in the $H_{\rm obs} = H_1 + H_2$ and $H_{\rm obs} = H_2 + H_3$ scenarios, this condition was imposed on H_2, since in both these scenarios it is typically the Higgs boson with SM-like couplings. The total number of points, $N_{\rm total}$, remaining after this filter is given in Table 2 for each scenario considered. All these points were then tested for consistency with the LEP and LHC exclusion limits on the other, non-SM-like, Higgs bosons of the model, using the package HiggsBounds v4.2.0 [80–83]. The points passing the HiggsBounds test were retained as the "good points" for further analysis, and their number, denoted by $N_{\rm HB}$, for each scenario is also given in Table 2. We point out for later reference that in each of the two $H_{\rm obs} = H_1$ scenarios and $H_{\rm obs} = H_1 + H_2$ scenario, the number of surviving good points (where they are available) is very identical across all input values of ϕ_κ, implying mutually fairly consistent sample sizes.

Next we carried out fits to $H_{\rm obs}$ data for the good points using the public code HiggsSignals v1.3.2 [73]. For obtaining these fits, HiggsSignals requires, along with the masses and BRs of each Higgs boson, H_i, the square of its normalised effective couplings, $(g_{H_iX}/g_{h_{\rm SM}X})^2$, to a given SM particle pair X, with $h_{\rm SM}$ being the SM Higgs boson with the same mass as H_i. Note that when X is a pair of fermions, there is a scalar as well as a pseudoscalar normalised coupling for each H_i, both of which need to be passed separately to HiggsSignals. All these are then used to calculate the normalised cross sections:

$$\mu^X_{H_i} \equiv \frac{\sigma\left(pp \longrightarrow H_i \longrightarrow X\right)}{\sigma\left(pp \longrightarrow h_{\rm SM} \longrightarrow X\right)}, \tag{10}$$

corresponding to a given decay channel, X, in an approximate way. The NMSSMCALC version we used did not provide the normalised Higgs boson couplings as an output. We therefore modified the code to obtain these couplings for adding them as a dedicated block in the SLHA input file for HiggsSignals.

The program HiggsSignals compares the computed $\mu^X_{H_i}$ for each H_i with the experimentally measured ones, $\mu^X_{\rm exp}$, for wide ranges of input Higgs boson masses in a variety of its production and decay channels at the LHC and the Tevatron. We used only the "peak-centred" method and the "latestresults" observable set in the program, with the assignment range variable Λ set to the default value of 1. It thus performed a fit to a total of 81 Higgs boson peak observables (77 from signal strength and 4 from mass measurements), from the CMS, ATLAS, CDF, and DØ collaborations, for a given model point. We assumed a Gaussian theoretical uncertainty of 2 GeV in the masses of the three lightest neutral Higgs bosons of the model. The default values of the uncertainties in the Higgs boson production cross sections as well as BRs were retained. Further details about the fitting procedure can be found in the manual [73] of the package. The main output of HiggsSignals contains the total χ^2 and the p value from the fit, given the number of statistical degrees of freedom, for each model point. Since the aim of this study is a comparison of various $H_{\rm obs}$ scenarios rather than the overall goodness of fit for each, we will quantify our results only in terms of χ^2 and ignore p value.

As an observable indication of the presence of more than one Higgs boson near 125 GeV, the double ratios

$$D_1 = \frac{R^h_{\rm VBF}\left(\gamma\gamma\right)/R^h_{gg}\left(\gamma\gamma\right)}{R^h_{\rm VBF}\left(bb\right)/R^h_{gg}\left(bb\right)};$$

Table 2: Number of scanned points remaining after imposing the mass constraint on $H_{\rm obs}$ and those passing the HiggsBounds test, for each scenario studied. See text for details.

Scenario	Low-λ	$H_{\rm obs} = H_1$	$H_{\rm obs} = H_2$	$H_{\rm obs} = H_3$	$H_{\rm obs} = H_1 + H_2$	$H_{\rm obs} = H_2 + H_3$
			$\phi_\kappa = 0^\circ$			
$N_{\rm total}$	17786	15675	15072	14431	26045	23736
$N_{\rm HB}$	17722	13691	2904	965	11878	2819
			$\phi_\kappa = 3^\circ$			
$N_{\rm total}$	17829	15775	15026	14806	27199	25684
$N_{\rm HB}$	17782	13885	3235	2391	11863	1659
			$\phi_\kappa = 10^\circ$			
$N_{\rm total}$	17847	15784	15080	14810	26735	28348
$N_{\rm HB}$	17786	13866	2411	2495	12607	3369
			$\phi_\kappa = 30^\circ$			
$N_{\rm total}$	17810	16256	15037	14671	31719	28685
$N_{\rm HB}$	17743	14725	247	276	13503	2012
			$\phi_\kappa = 60^\circ$			
$N_{\rm total}$	17810	0	14996	14438	0	30412
$N_{\rm HB}$	17743	0	247	2	0	242

$$D_2 = \frac{R^h_{\rm VBF}(\gamma\gamma)/R^h_{gg}(\gamma\gamma)}{R^h_{\rm VBF}(WW)/R^h_{gg}(WW)};$$
$$D_3 = \frac{R^h_{\rm VBF}(WW)/R^h_{gg}(WW)}{R^h_{\rm VBF}(bb)/R^h_{gg}(bb)} \tag{11}$$

were proposed in [74]. Each of these ratios should be unity if $H_{\rm obs}$ consists of only a single Higgs boson, while the contribution of two (or more) Higgs bosons to $H_{\rm obs}$ signal could result in a deviation of these ratios from 1. In the above expressions, $R^h_Y(X) = R^{H_i}_Y(X) + R^{H_j}_Y(X)$, where H_i and H_j are the two mass-degenerate Higgs bosons in a given scenario and the subscripts VBF and gg imply the vector boson fusion and the gluon fusion production modes, respectively. $R^{H_i}_Y(X)$ for each H_i is defined as

$$R^{H_i}_Y(X) \equiv \frac{\Gamma(H_i \longrightarrow Y)}{\Gamma(h_{\rm SM} \longrightarrow Y)} \times \frac{{\rm BR}(H_i \longrightarrow X)}{{\rm BR}(h_{\rm SM} \longrightarrow X)} = \frac{C^{H_i}_Y C^{H_i}_X}{\Gamma_{H_i}/\Gamma_{h_{\rm SM}}}, \tag{12}$$

with Y being the given production mode and, in the last equality, $C^{H_i}_{X(Y)} = \Gamma(H_i \to X(Y))/\Gamma(h_{\rm SM} \to X(Y))$, the normalised partial decay width of H_i into $X(Y)$ pair. (Note that (12) assumes that $h_{\rm SM}$-normalised production cross sections for Y = VBF and gg processes can be approximated by the normalised partial decay widths of H_i in VV and gg decay channels, resp.) Γ_{H_i} and $\Gamma_{h_{\rm SM}}$ are the total decay widths of H_i and $h_{\rm SM}$, respectively.

We also evaluated the ratios D_1, D_2, and D_3 for the points which give reasonably good fits to the data (to be defined later) in the scenarios with two mass-degenerate Higgs bosons. For this purpose, $R^{H_i}_Y(X)$ for each H_i was calculated by fixing $\Gamma_{h_{\rm SM}}$ in (12) to 4.105×10^{-3} GeV, which is the value given by the program HDECAY [84] for 125 GeV $h_{\rm SM}$. A change of ± 2 GeV in the mass of $h_{\rm SM}$ has only a marginal effect on this width, which we ignore. For calculating the $\Gamma_{h_{\rm SM}}$ with HDECAY, care was taken that all the partial decay widths of $h_{\rm SM}$ were evaluated at the same perturbative order as that implemented in NMSSMCALC for computing Γ_{H_i}. Moreover, $C^{H_i}_Y$ is simply the squared normalised coupling of H_i to a vector boson, V, pair for the VBF production mode and to a gluon pair for gg mode. Similarly, $C^{H_i}_X$ implies H_iVV and $H_i\gamma\gamma$ normalised couplings squared, respectively, for $X = WW$ and $\gamma\gamma$. All these couplings are thus the same ones obtained from NMSSMCALC for passing to HiggsSignals. In the case of $X = b\bar{b}$, though, there is a scalar and pseudoscalar coupling for each H_i, as noted above. For this reason, $C^{H_i}_{b\bar{b}}$'s were calculated using the actual $\Gamma(H_i \to b\bar{b})$ from the NMSSMCALC output for a given model point and $\Gamma(h_{\rm SM} \to b\bar{b})$ obtained from HDECAY for $m_{h_{\rm SM}} = 125$ GeV.

4. Results and Discussion

In Figure 1 we show the total χ^2 obtained for the points from our scans for the various $H_{\rm obs}$ scenarios considered. The green points in the figure correspond to $\phi_\kappa = 0^\circ$, violet to $\phi_\kappa = 3^\circ$, blue to $\phi_\kappa = 10^\circ$, red to $\phi_\kappa = 30^\circ$, and cyan to $\phi_\kappa = 60^\circ$. For the scenarios in which only one of the three lightest neutral Higgs bosons is assumed to be $H_{\rm obs}$, we have made sure that the difference between the mass of $H_{\rm obs}$ and that of each additional Higgs boson nearest to it is always larger than 2.5 GeV. The lower cut-off in χ^2 in each panel, in this figure and in those that follow, varies depending on the minimum value obtained in the corresponding scenario. The upper cut-off in χ^2 for each scenario is chosen so as to include as many points in the corresponding figures as possible without χ^2 getting more than 10 units larger than the minimum obtained in that scenario (given that there are 9 statistical degrees of freedom).

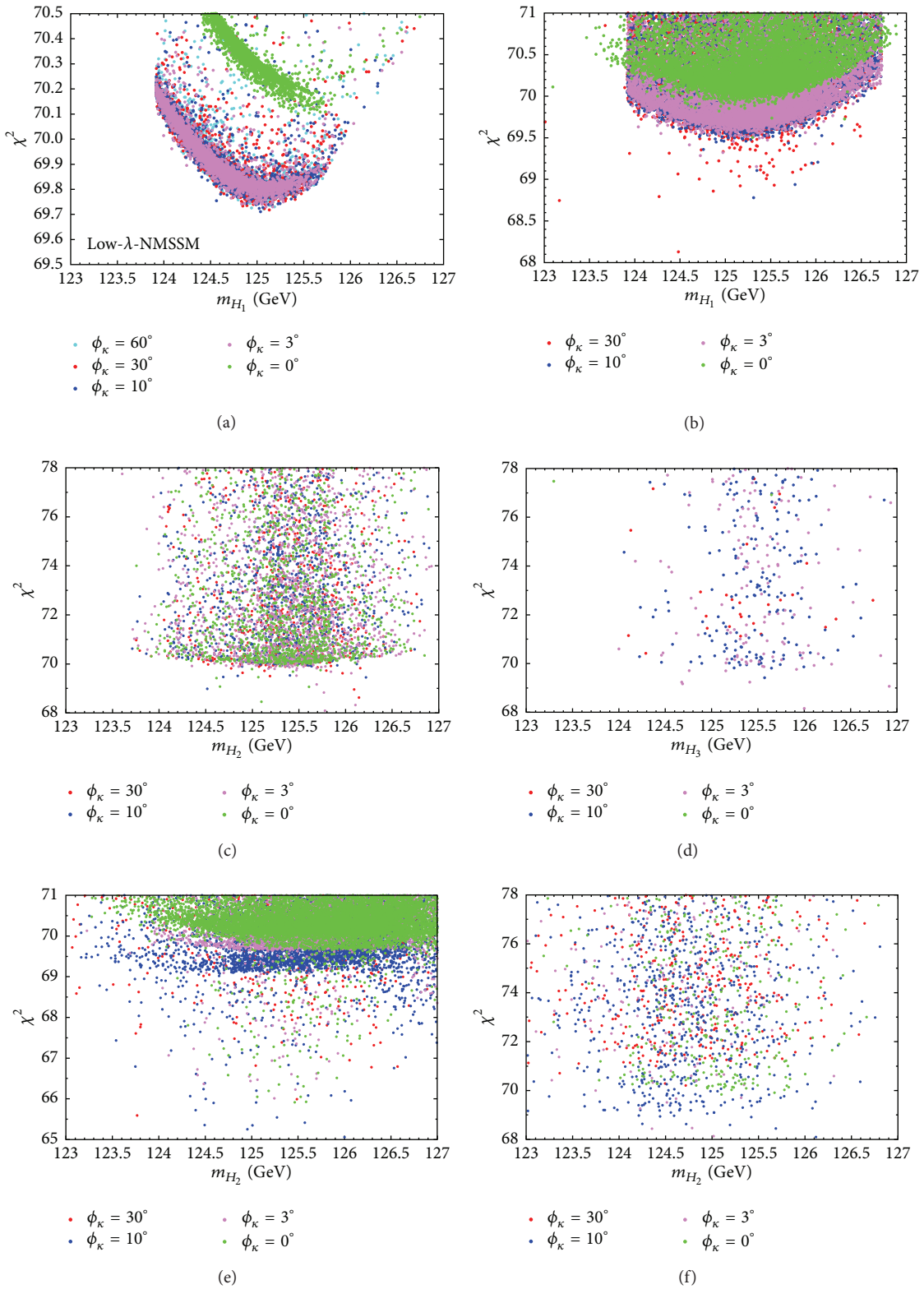

FIGURE 1: Total χ^2 as a function of the following: ((a), (b)) m_{H_1} when only H_1 is assumed to be H_{obs}, for two different sets of scanned ranges of the parameter space (see text for details); (c) m_{H_2} when only H_2 is the H_{obs}; (d) m_{H_3} when only H_3 is H_{obs}; (e) m_{H_2} when both H_1 and H_2 lie near 125 GeV; and (f) m_{H_2} when both H_2 and H_3 lie near 125 GeV.

Figure 1(a) corresponds to the low-λ-NMSSM scenario. One notices in the figure that, for $\phi_\kappa = 0^\circ$, $\chi^2_{\min}$ lies very close to 70 and is thus almost identical to $\chi^2_{\min} = 69.96$ that is given by HiggsSignals for a SM Higgs boson at a mass of 125.1 GeV, with the same settings as those used by us. The input parameters (with the exception of M_0, $M_{1/2}$, and A_0, which can be adjusted with much more freedom) and the masses of the three lightest Higgs bosons are given in Table 3. The negligibly small difference in $\chi^2_{\min}$ value obtained for $h_{\rm SM}$ and for the CP-conserving low-λ-NMSSM results from the fact that λ for the corresponding point in the latter is nonvanishing, as seen in the table, so that the singlet sector is not completely decoupled and an exact MSSM limit is not reached. One can notice in the figure and the table a slightly lower value of $\chi^2_{\min}$ obtained for the sets of points corresponding to nonzero ϕ_κ values. However, λ for all these points is even larger than in the CP-conserving limit. Note also that, for all ϕ_κ, most of the points give $\Delta\chi^2 \leq 1$.

In Figure 1(b), which corresponds to $H_{\rm obs} = H_1$ scenario in the natural NMSSM, we see that there is a large concentration of points above χ^2 value which is very similar to $\chi^2_{\min}$ seen in Figure 1(a), for each corresponding ϕ_κ. For nonzero ϕ_κ though, one also sees a few scattered points with χ^2 lower than that for any of the points in the high concentration region. The overall lowest χ^2 lies very close to 68, for $\phi_\kappa = 30^\circ$, with the mass of $H_{\rm obs}$ for the corresponding point lying at 124.5 GeV. However, according to Table 3, the mass of H_2 for this point is within 3 GeV of that of H_1. It is therefore very likely that the relatively better fit for this particular point is a result of the assignment of H_2 instead of or along with H_1 to some of the observables, especially when their experimental mass resolution is relatively poor. This possibility, which implies that our assumption of two Higgs bosons being individually irresolvable if their masses lie within 2.5 GeV of each other is rather robust, will be discussed further later. For $\phi_\kappa = 60^\circ$ none of the points obtained in the scan for this scenario had H_1 heavier than 123 GeV.

In $H_{\rm obs} = H_2$ scenario, a much smaller number of points were passed by HiggsBounds compared to $H_{\rm obs} = H_1$ scenario, as seen in Figure 1(c), but $\chi^2_{\min}$ is equally low for most ϕ_κ here, including 0°. Only for $\phi_\kappa = 60^\circ$, while plenty of points with $m_{H_2} \approx 125$ GeV were obtained in the scan, χ^2 for them is never low enough to appear in the figure. Once again, in Table 3 one can see that, for the points giving the lowest χ^2 for each ϕ_κ in this scenario, H_1 always lies within 3-4 GeV of H_2. Hence the slightly better fit for this point is again made possible by a contribution of H_1 to some search channels. In Figure 1(d) for $H_{\rm obs} = H_3$ scenario, although very few points with $\Delta\chi^2 < 10$ appear in this scenario compared to the ones above, $\chi^2_{\min}$ is very similar, except for $\phi_\kappa = 0^\circ$ case, when it has a fairly high value of around 77.

In Figure 1(e) is shown the total χ^2 for $H_{\rm obs} = H_1 + H_2$ scenario against H_2 mass. One can observe quite a few similarities between this figure and Figure 1(b) seen above (for $H_{\rm obs} = H_1$ scenario). There are once again a large concentration of points with $\chi^2 \gtrsim 69$ for all ϕ_κ except 60° and also many scattered points below it. Importantly though, there are many points in this scenario which give χ^2 lower than 68, which is the overall lowest value observed for any other scenario here. Most of these points, including the one with the overall lowest χ^2 of ~65, correspond to $\phi_\kappa = 10^\circ$, although some points for other ϕ_κ can also be noticed. In Figure 1(f) one sees $\chi^2_{\min}$ of 68 for $H_{\rm obs} = H_2 + H_3$ scenario also but very few points with $\chi^2 < 71$, in contrast with $H_{\rm obs} = H_1$ and $H_{\rm obs} = H_1 + H_2$ scenarios but similar to $H_{\rm obs} = H_2$ and $H_{\rm obs} = H_3$ scenarios.

From the above discussion, it is clear that certain points, or parameter space configurations, in $H_{\rm obs} = H_1 + H_2$ scenario give the best fit to the current experimental Higgs boson data. A *global* $\chi^2_{\min}$, that is, the lowest χ^2 value across all scenarios examined here, of around 65 has been observed for $\phi_\kappa = 10^\circ$ in this scenario, with some points corresponding to other values of ϕ_κ also lying within 1 unit of χ^2. None of the points obtained for the other scenarios gives χ^2 lying even within 3 units of this global minimum, despite the number of sampled points for the $H_{\rm obs} = H_1$ scenario being typically larger. The reason for a better fit for some points with two nearly degenerate Higgs bosons becomes apparent by looking at the detailed output of HiggsSignals. In the peak-centred method, HiggsSignals assigns to a given observable the Higgs boson with a mass closest to the measured mass provided by the experiment. This mass measurement currently ranges between 124.7 GeV and 126.0 GeV. Thus, when a single Higgs boson is assigned to all the observables, χ^2 contribution is large from the observables for which the measured mass lies away from the mass of the assigned Higgs boson, and the experimental mass resolution is good. On the other hand, when two Higgs bosons lie close to each other, the one assigned to a given observable is the one for which the difference of the predicted mass from the experimental value is the smallest, so that χ^2 contribution from this observable is minimal. This is as long as the mass of the other Higgs boson nearby lies outside the experimental mass resolution; otherwise HiggsSignals automatically assigns both the Higgs bosons to an individual observable if it improves the fit.

Some caveats are in order here though. $\Delta\chi^2 \simeq 3$ is statistically quite insignificant for drawing any concrete inferences about the considered scenarios, since the total number of observables and statistical degrees of freedom is quite large. At the same time, the number of points giving $\Delta\chi^2 \leq 3$ is also fairly small. Moreover, no other experimental constraints have been imposed in our analysis, since the publicly available tools for testing these are so far not compatible with the cNMSSM. It is thus possible that many of the interesting points may have already been ruled out by such constraints. However, the aim of this study is not to disregard one scenario in favour of another, but to simply show that, given the current experimental data, the scenario with two mass-degenerate Higgs bosons in the NMSSM provides as good, if not better, a fit as the scenarios with a single Higgs boson near 125 GeV. This alternative possibility even points towards a source of CP-violation beyond the SM and, therefore, warrants more dedicated analyses as well as experimental probes. In the following we discuss some other interesting aspects of this scenario.

In the left, middle, and right panels of Figure 2 we show the ratios D_1, D_2, and D_3, respectively, as functions of

Table 3: Input parameters and Higgs boson masses corresponding to the points giving the lowest χ^2 for all ϕ_κ cases in each of $H_{\rm obs}$ scenarios considered.

Scenario	Low-λ	$H_{\rm obs} = H_1$	$H_{\rm obs} = H_2$	$H_{\rm obs} = H_3$	$H_{\rm obs} = H_1 + H_2$	$H_{\rm obs} = H_2 + H_3$
			$\phi_\kappa = 0^\circ$			
$\chi^2_{\rm min}$	70.1	69.5	68.5	76.9	65.9	69.8
λ	0.046	0.582	0.653	0.48	0.597	0.597
κ	0.213	0.43	0.511	0.305	0.302	0.327
$\tan\beta$	17.65	1.66	3.6	6.98	2.39	2.07
A_λ	853.6	226.8	609.7	680.7	540.0	179.3
A_κ	−2352	−741.4	−666.0	14.05	−479.3	−3.95
$\mu_{\rm eff}$	130.0	281.5	243.7	102.6	285.2	112.3
m_{H_1}	125.4	125.3	122.1	66.8	123.3	115.1
m_{H_2}	162.8	142.1	125.1	121.0	125.5	125.1
m_{H_3}	1828	510.6	618.5	125.7	730.0	126.6
			$\phi_\kappa = 3^\circ$			
$\chi^2_{\rm min}$	69.7	69.2	68.1	68.2	66.0	68.1
λ	0.184	0.639	0.588	0.662	0.631	0.636
κ	0.291	0.523	0.39	0.349	0.373	0.318
$\tan\beta$	29.6	1.81	2.61	4.24	1.61	6.45
A_λ	2175	162.5	459.6	425.6	222.0	848.6
A_κ	−236.7	−595.1	−597.6	−12.03	345.2	−19.4
$\mu_{\rm eff}$	177.9	218.8	260.5	110.1	196.4	127.4
m_{H_1}	125.1	125.3	122.5	97.2	123.4	105.1
m_{H_2}	444.9	141.7	125.8	122.3	125.2	125.0
m_{H_3}	496.1	405.5	563.6	126.0	366.3	127.2
			$\phi_\kappa = 10^\circ$			
$\chi^2_{\rm min}$	69.7	68.8	69.0	69.4	65.1	68.1
λ	0.138	0.68	056	0.692	0.688	0.585
κ	0.219	0.409	0.345	0.338	0.361	0.306
$\tan\beta$	16.7	1.85	1.91	4.88	1.98	7.55
A_λ	1379	291.6	347.8	557.0	390.8	972.6
A_κ	−623.8	−476.1	−567.8	12.7	−435.1	−30.62
$\mu_{\rm eff}$	133.5	251.0	266.9	124.3	254.0	136.7
m_{H_1}	125.0	125.3	120.3	106.4	123.6	118.7
m_{H_2}	212.2	140.5	124.5	111.6	126.0	126.1
m_{H_3}	631.6	482.5	541.8	125.6	440.1	127.4
			$\phi_\kappa = 30^\circ$			
$\chi^2_{\rm min}$	69.7	68.1	68.6	70.4	65.6	70.2
λ	0.136	0.648	0.679	0.537	0.624	0.481
κ	0.219	0.319	0.586	0.303	0.388	0.311
$\tan\beta$	29.4	2.2	2.13	6.55	2.10	7.67
A_λ	3515	570.1	295.0	702.2	345.7	796.5
A_κ	−781.0	−398.4	−590.7	7.07	330.5	−23.22
$\mu_{\rm eff}$	170.8	288.5	227.8	112.6	209.1	110.0
m_{H_1}	125.1	124.5	123.1	86.5	121.6	107.1
m_{H_2}	234.3	127.4	126.1	116.8	123.8	124.7
m_{H_3}	857.7	462.4	507.8	124.3	405.8	125.8

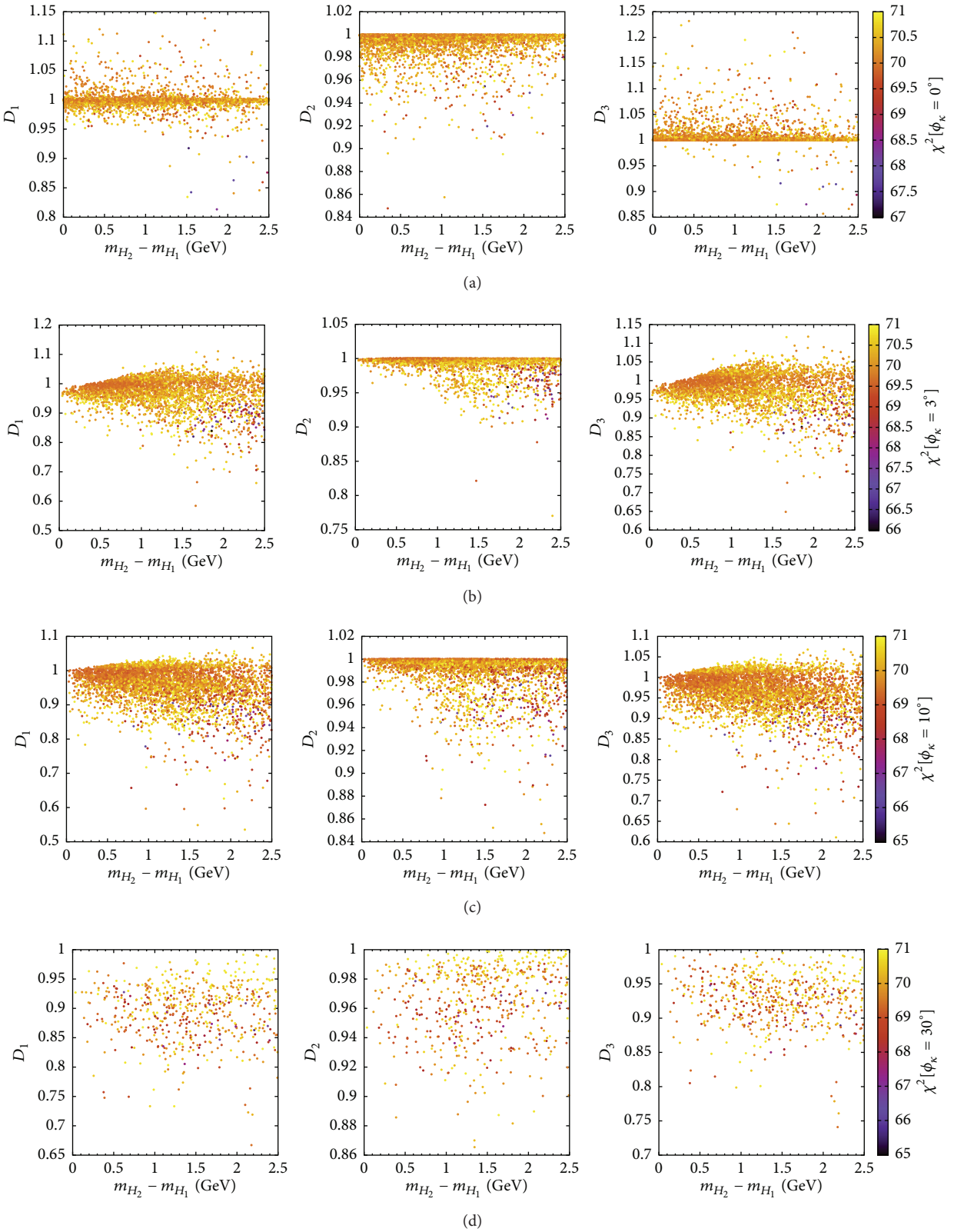

FIGURE 2: The ratios D_1, D_2, and D_3, defined in (11), as functions of the difference between H_2 and H_1 masses, in the scenario when $H_{\text{obs}} = H_1 + H_2$. In (a) ϕ_κ is set to 0°, in (b) to 3°, in (c) to 10°, and in (d) to 30°. The heat map in all the panels corresponds to the total χ^2.

the mass difference, $m_{H_2} - m_{H_1}$, for various ϕ_κ values in $H_{\rm obs} = H_1 + H_2$ scenario. The heat map corresponds to the total χ^2 obtained for the points shown in each panel. χ^2 has a uniform upper cut-off of 71 across all panels, as in Figure 1(e), but its lower cut-off varies according to the minimum obtained for ϕ_κ case that a given panel corresponds to. According to Figure 2(a), for $\phi_\kappa = 0^\circ$ the three ratios remain largely close to unity, but deviations up to 15–20% can be seen for some points. D_2, the ratio dependent on only the bosonic signal strengths, only gets smaller than 1 for some points and its maximum observed deviation is lower than that of D_1 and D_3, each of which can be both above or below unity. Importantly, the points for which a large deviation of each ratio from 1 is seen are also generally the ones giving a relatively good χ^2 fit to the data.

A similar trend is seen also for other values of ϕ_κ. However, deviations of D_1 and D_2 from unity by up to 40–50% are obtained for $\phi_\kappa = 3^\circ$ (Figure 2(b)) and $\phi_\kappa = 10^\circ$ (Figure 2(c)), but there are many more points with significantly large deviations of each of the ratios for the latter phase compared to the former one. For $\phi_\kappa = 30^\circ$ all the points appearing in Figure 2(d) give D_1, D_2, and D_3 smaller than 1 and the overall deviation is generally smaller than for other nonzero phases but larger than for the rNMSSM limit. Thus, for this phase, the measured signal strengths can provide a clear indication whenever two Higgs bosons are present near 125 GeV instead of one. The reason why the deviations of the three ratios are much smaller overall in the case of $\phi_\kappa = 0^\circ$ than for the CPV cases, for points showing the highest consistency with the data, will become clearer below.

As noted earlier, a scenario with two mass-degenerate Higgs bosons in the cNMSSM entails both $H_{\rm obs} = H_1 + H_2$ and $H_{\rm obs} = H_1/H_2 + A_1$ possibilities of the rNMSSM. Thus it is interesting to see which one of these two possibilities is favoured more by the data, for a given ϕ_κ. In the left panels of Figure 3 we thus show the squared normalised coupling $C_{VV}^{H_2}$ against $C_{VV}^{H_1}$, with the heat map corresponding to the total χ^2. Similarly, in the right panels we have plotted $C_{VV}^{H_3}$ versus $C_{VV}^{H_1}$, while the distribution of m_{H_3} is shown by the heat map. For clarity of observation, we have included in this figure points with a total χ^2 reaching up to 80, which is much higher than for the points shown in the earlier figures for this scenario. Also we have imposed an upper cut-off of 300 GeV on the mass of H_3. We expect $C_{VV}^{H_i}$ to either vanish when a given H_i is a pure pseudoscalar (in the rNMSSM limit) or be relatively small when it is pseudoscalar-like (for $\phi_\kappa > 0^\circ$). Note that these couplings satisfy the sum rule [63, 64]

$$\sum_{i=1}^{N} C_{VV}^{H_i} \simeq 1, \tag{13}$$

where N is the total number of neutral Higgs bosons that have a tree-level coupling to the gauge bosons, that is, 5 in the cNMSSM and 3 in the rNMSSM limit. (Note that since $h_{\rm SM}$ is a hypothetical SM Higgs boson with the same mass as a given H_i, at the tree level the ratio $C_X^{H_i}$ in fact corresponds to $(g_{H_iX}/g_{h_{\rm SM}X})^2$ and the equality in (13) is exact. However, since $C_X^{H_i}$ have actually been defined here in terms of the partial decay widths of H_i in X channel, which include higher order effects also, the sum of $C_X^{H_i}$ may deviate slightly from unity.) In the figure we see the above sum rule being satisfied almost completely by the three lightest neutral Higgs bosons under consideration here, implying that the remaining two doublet-like Higgs bosons are nearly decoupled.

In the case of $\phi_\kappa = 0^\circ$ (i.e., in the rNMSSM limit) in the left panel of Figure 3(a), we see two distinct kinds of points. There are some points lying along the diagonal, for which $C_{VV}^{H_1}$ and $C_{VV}^{H_2}$ alone are enough to satisfy the sum rule in (13). It is further evident from the right panel that $C_{VV}^{H_3}$ for these points is exactly 0. H_1 and H_2 in these points should thus be scalars and H_3 should be a pseudoscalar (i.e., A_1). But for the majority of the points, lying along either of the axes, $C_{VV}^{H_1}$ is nearly 1, implying it is an almost pure doublet-like scalar, while $C_{VV}^{H_2}$ is exactly 0, implying it is a pseudoscalar, or vice versa. One can then observe in the right panel that for such points $C_{VV}^{H_3}$, with H_3 being the singlet-like scalar, is responsible for the sum rule being satisfied. Thus when the doublet-like scalar, whether H_1 or H_2, has $C_{VV}^{H_i}$ slightly below 1, $C_{VV}^{H_3}$ is slightly above 0. The mixing of the doublet scalar with H_3 increases as its mass decreases, as is evident from the heat map in the right panel of the figure. As a result, the largest $C_{VV}^{H_3}$, ~0.8, is seen for the lowest m_{H_3} obtained, which lies just above the allowed $H_{\rm obs}$ mass window.

A closer inspection of the heat map in the left panel of Figure 3(a) reveals that the lowest values of χ^2 are obtained for points lying along one of the axes, that is, when the doublet-like scalar is nearly mass-degenerate with the pseudoscalar. For points along the diagonal, χ^2 is in fact always larger than 71. This is the reason for the relatively small deviations of D_1, D_2, and D_3 from 1 seen in Figure 2(a), where only points with χ^2 lower than 71 were shown. For such points, since one of H_1 and H_2 is a pure pseudoscalar as well as singlet-dominated, its contribution to the combined signal strength in WW channel is null and that in $\gamma\gamma$ and $b\bar{b}$ channels is minimal. Therefore, while the presence of H_1 and H_2 of the rNMSSM near 125 GeV may possibly cause D_1, D_2, and D_3 to deviate more significantly from 1, the consistency of this scenario with the LHC data is worse than that of $H_1 + A_1$ scenario.

Figure 3(b) shows that, for $\phi_\kappa = 3^\circ$, H_1 and H_2 are almost always scalar-like while H_3 is highly pseudoscalar-like with a relatively much smaller $C_{VV}^{H_3}$ generally. However, due to CP-mixing, $C_{VV}^{H_3}$ can reach as high as 0.7 or so when the mass of H_3 is close to that of H_1 and H_2, though this happens for only a few points. A very crucial point to note here is that the total χ^2 in the left panel never falls below 68, which is due to the cut-off on the allowed upper value of m_{H_3}. This means that the points which give the overall best fit to the data have a much higher H_3 mass, which leads to a much smaller scalar-pseudoscalar mixing and hence negligible $C_{VV}^{H_3}$.

For $\phi_\kappa = 10^\circ$ case, illustrated in Figure 3(c), while the maximum $C_{VV}^{H_3}$ obtained is relatively small and hence $C_{VV}^{H_1}$ and $C_{VV}^{H_2}$ do not deviate from the diagonal by much in the left panel, there are many more points, compared to $\phi_\kappa = 3^\circ$

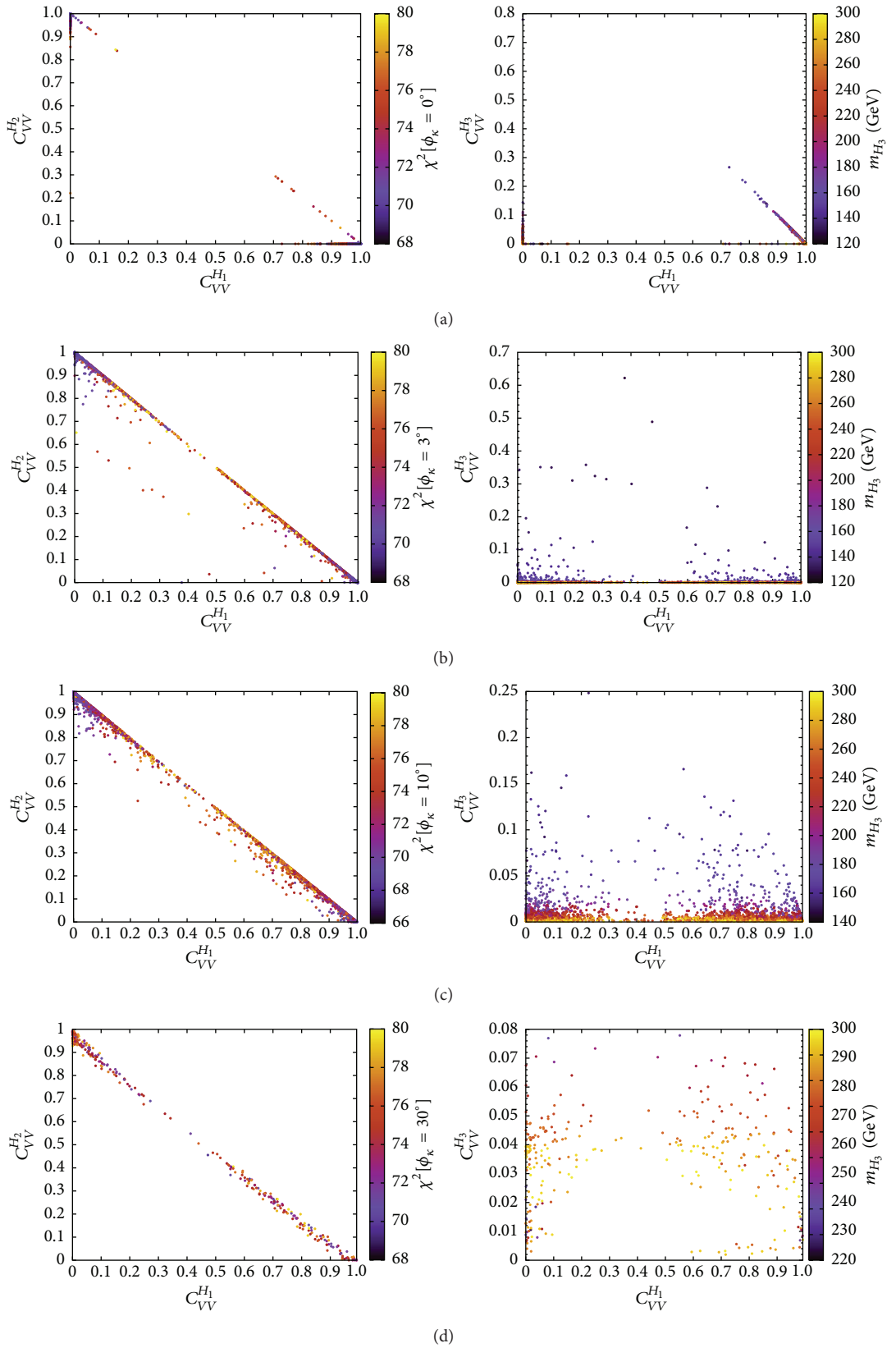

FIGURE 3: Squared normalised coupling of H_1 to the gauge bosons versus that of H_2 (left) and of H_3 (right) in the scenario when $H_{\text{obs}} = H_1 + H_2$, with ϕ_κ set to (a) 0°, (b) 3°, (c) 10°, and (d) 30°. The heat map in the left panels shows the distribution of χ^2 and in the right panels that of m_{H_3}.

case above, for which $C_{VV}^{H_3}$ is significant, according to the right panel. Finally, for $\phi_\kappa = 30^\circ$, although $C_{VV}^{H_3}$ never completely vanishes, it also stays smaller overall than it is for other phases. The reason for this is that the pseudoscalar-like H_3 never achieves a mass below 220 GeV or so, as can be noted from the heat map in the right panel of Figure 3(d). In the left panel one therefore sees that $C_{VV}^{H_1}$ and $C_{VV}^{H_2}$ always remain very close to the diagonal. Hence, for nonzero ϕ_κ the data clearly favours two scalar-like Higgs bosons near 125 GeV, instead of a pair of scalar-like and pseudoscalar-like Higgs bosons.

5. Conclusions

In summary, we have tested the consistency of the real and complex NMSSM with the latest Higgs boson data from the LHC Run I and the Tevatron. In particular, we have focused on scenarios wherein the resonant peak seen by the experiments can be explained in terms of two nearly mass-degenerate Higgs states around 125 GeV. Such scenarios have been verified in the rNMSSM previously and have not been ruled out yet. What we have shown here is that the possibility of such dynamics being available in the NMSSM is somewhat enhanced if some degree of (explicit) CP-violation is allowed in the Higgs sector. This can be done by assuming one or more of the Higgs sector parameters to be complex. By choosing this parameter to be κ, one can evade the fermion EDM measurements, which tightly constrain the other possibly complex parameters in the Higgs and soft SUSY sectors of the NMSSM.

In order to achieve the above we have performed detailed numerical scans of the parameter space of the cNMSSM to obtain various possible configurations with ~125 GeV Higgs boson(s) that also give SM-like signal strengths. In these scans we set the phase of κ to five different values, 0°, 3°, 10°, 30°, and 60°. Through a comprehensive analysis of the points obtained from these scans, we have then established that certain parameter configurations yielding two Higgs bosons near 125 GeV are slightly more favoured by the current data compared to scenarios with a single ~125 GeV Higgs boson. This statement is even stronger when the two Higgs bosons are CP-mixed states. For the case of $\phi_\kappa = 10^\circ$ we thus obtained the following: (i) the point with the global minimum χ^2; (ii) more points with $\Delta\chi^2$ lying within 4 units of the global minimum χ^2 compared to all other scenarios and phases tested; (iii) more points with larger deviations of the ratios D_1, D_2, and D_3 from unity.

While analysing the aforementioned scenario with two Higgs bosons near 125 GeV, we have made sure that their masses are close enough that these two states cannot be distinguished experimentally as separate particles. In doing so we have exploited the fact that the experimental measurements are currently unable to reconstruct Breit-Wigner resonances, given that the experimental resolution in all channels investigated in the Higgs analyses is significantly larger than the intrinsic Higgs boson widths involved (so that LHC data actually reproduce Gaussian shapes). However, (tree-level) interference and (1-loop) mixing effects become crucial and need to be accounted for when the (pole) mass difference between two Higgs states is comparable or smaller that their individual intrinsic width. While we have ignored such effects here for points where they can be relevant, which however make up a very tiny fraction of all the good points from our scans, they are the subject of a dedicated separate study [85].

Finally, in our analysis we have used up-to-date sophisticated computational tools in which state-of-the-art theoretical calculations and/or experimental measurements have been implemented, so that the solidity of our results is assured.

Conflict of Interests

The authors declare that there is no conflict of interests regarding the publication of this paper.

Acknowledgments

Shoaib Munir is thankful to Margarete Mühlleitner for useful discussions regarding the cNMSSM and for help with the NMSSMCALC program. Stefano Moretti is supported in part by the NExT Institute. Shoaib Munir is supported by Korea Ministry of Science, ICT and Future Planning, Gyeongsangbuk-Do, and Pohang City for Independent Junior Research Groups at the Asia Pacific Center for Theoretical Physics.

References

[1] P. Fayet, "Supergauge invariant extension of the Higgs mechanism and a model for the electron and its neutrino," *Nuclear Physics B*, vol. 90, pp. 104–124, 1975.

[2] J. Ellis, J. F. Gunion, H. E. Haber, L. Roszkowski, and F. Zwirner, "Higgs bosons in a nonminimal supersymmetric model," *Physical Review D*, vol. 39, article 844, 1989.

[3] L. Durand and J. L. Lopez, "Upper bounds on Higgs and top quark masses in the flipped SU(5)×U(1) superstring model," *Physics Letters B*, vol. 217, no. 4, pp. 463–466, 1989.

[4] M. Drees, "Supersymmetric models with extended Higgs sector," *International Journal of Modern Physics A*, vol. 4, no. 14, article 3635, 1989.

[5] U. Ellwanger, C. Hugonie, and A. M. Teixeira, "The next-to-minimal supersymmetric standard model," *Physics Reports*, vol. 496, no. 1-2, pp. 1–77, 2010.

[6] M. Maniatis, "The next-to-minimal supersymmetric extension of the standard model reviewed," *International Journal of Modern Physics A*, vol. 25, pp. 3505–3602, 2010.

[7] G. Aad, T. Abajyan, B. Abbott et al., "Observation of a new particle in the search for the Standard Model Higgs boson with the ATLAS detector at the LHC," *Physics Letters B*, vol. 716, no. 1, pp. 1–29, 2012.

[8] S. Chatrchyan, V. Khachatryan, A. M. Sirunyan et al., "Observation of a new boson at a mass of 125 GeV with the CMS experiment at the LHC," *Physics Letters B*, vol. 716, no. 1, pp. 30–61, 2012.

[9] S. Chatrchyan, V. Khachatryan, A. M. Sirunyan et al., "Observation of a new boson with mass near 125 GeV in pp collisions at $\sqrt{s} = 7$ and 8 TeV," *Journal of High Energy Physics*, vol. 2013, no. 6, article 081, 2013.

[10] U. Ellwanger, "A Higgs boson near 125 GeV with enhanced diphoton signal in the NMSSM," *Journal of High Energy Physics*, vol. 2012, no. 3, article 44, 2012.

[11] S. F. King, M. Mühlleitner, and R. Nevzorov, "NMSSM Higgs benchmarks near 125 GeV," *Nuclear Physics B*, vol. 860, no. 2, pp. 207–244, 2012.

[12] J. Cao, Z. Heng, J. M. Yang, Y. Zhang, and J. Zhu, "A SM-like Higgs near 125 GeV in low energy SUSY: a comparative study for MSSM and NMSSM," *Journal of High Energy Physics*, vol. 2012, article 86, 2012.

[13] J. F. Gunion, Y. Jiang, and S. Kraml, "Could two NMSSM Higgs bosons be present near 125 GeV?" *Physical Review D*, vol. 86, no. 7, Article ID 071702, 2012.

[14] S. King, M. Muhlleitner, R. Nevzorov, and K. Walz, "Natural NMSSM Higgs bosons," *Nuclear Physics B*, vol. 870, pp. 323–352, 2013.

[15] T. Gherghetta, B. von Harling, A. D. Medina, and M. A. Schmidt, "The scale-invariant NMSSM and the 126 GeV Higgs boson," *Journal of High Energy Physics*, vol. 2013, no. 2, article 032, 2013.

[16] L. Wu, J. M. Yang, C.-P. Yuan, and M. Zhang, "Higgs self-coupling in the MSSM and NMSSM after the LHC Run 1," *Physics Letters B*, vol. 747, pp. 378–389, 2015.

[17] S. Munir, L. Roszkowski, and S. Trojanowski, "Simultaneous enhancement in gamma.gamma, b.b-bar and tau+.tau− rates in the NMSSM with nearly degenerate scalar and pseudoscalar Higgs bosons," *Physical Review D*, vol. 88, Article ID 055017, 2013.

[18] A. G. Cohen, D. Kaplan, and A. Nelson, "Progress in electroweak baryogenesis," *Annual Review of Nuclear and Particle Science*, vol. 43, pp. 27–70, 1993.

[19] M. Quiros, "Field theory at finite temperature and phase transitions," *Helvetica Physica Acta*, vol. 67, no. 5, pp. 451–583, 1994.

[20] A. Sakharov, "Violation of CP invariance, C asymmetry, and baryonasymmetry of the universe," *Pisma Zh.Eksp.Teor.Fiz*, vol. 5, pp. 32–35, 1967.

[21] T. Ibrahim and P. Nath, "*CP* violation from the standard model to strings," *Reviews of Modern Physics*, vol. 80, article 577, 2008.

[22] T. Cohen, D. E. Morrissey, and A. Pierce, "Electroweak baryogenesis and Higgs signatures," *Physical Review D*, vol. 86, Article ID 013009, 2012.

[23] D. Curtin, P. Jaiswal, and P. Meade, "Excluding electroweak baryogenesis in the MSSM," *Journal of High Energy Physics*, vol. 2012, no. 8, article 005, 2012.

[24] M. Carena, G. Nardini, M. Quiros, and C. E. Wagner, "MSSM electroweak baryogenesis and LHC data," *Journal of High Energy Physics*, vol. 2013, no. 2, article 001, 2013.

[25] A. Pilaftsis, "CP-odd tadpole renormalization of Higgs scalar-pseudoscalar mixing," *Physical Review D*, vol. 58, Article ID 096010, 1998.

[26] A. Pilaftsis, "Higgs scalar—pseudoscalar mixing in the minimal supersymmetric standard model," *Physics Letters B*, vol. 435, pp. 88–100, 1998.

[27] A. Pilaftsis and C. E. M. Wagner, "Higgs bosons in the minimal supersymmetric standard model with explicit CP violation," *Nuclear Physics B*, vol. 553, no. 1-2, pp. 3–42, 1999.

[28] M. S. Carena, J. R. Ellis, A. Pilaftsis, and C. E. M. Wagner, "Renormalization-group-improved effective potential for the MSSM Higgs sector with explicit CP violation," *Nuclear Physics B*, vol. 586, no. 1-2, pp. 92–140, 2000.

[29] S. Y. Choi, M. Drees, and J. S. Lee, "Loop corrections to the neutral Higgs boson sector of the MSSM with explicit CP violation," *Physics Letters B*, vol. 481, no. 1, pp. 57–66, 2000.

[30] M. S. Carena, J. R. Ellis, A. Pilaftsis, and C. Wagner, "Higgs boson pole masses in the MSSM with explicit CP violation," *Nuclear Physics B*, vol. 625, pp. 345–371, 2002.

[31] M. Carena, J. Ellis, S. Mrenna, A. Pilaftsis, and C. E. M. Wagner, "Collider probes of the MSSM Higgs sector with explicit CP violation," *Nuclear Physics B*, vol. 659, no. 1-2, pp. 145–178, 2003.

[32] S. Y. Choi, J. Kalinowski, Y. Liao, and P. M. Zerwas, "*H*/*A* Higgs mixing in *CP*-noninvariant supersymmetric theories," *European Physical Journal C*, vol. 40, no. 4, pp. 555–564, 2005.

[33] C. A. Baker, D. D. Doyle, P. Geltenbort et al., "Improved experimental limit on the electric dipole moment of the neutron," *Physical Review Letters*, vol. 97, no. 13, Article ID 131801, 2006.

[34] E. D. Commins, "Electric dipole moments of elementary particles, nuclei, atoms, and molecules," *Journal of the Physical Society of Japan*, vol. 76, no. 11, Article ID 111010, 2007.

[35] W. C. Griffith, M. D. Swallows, T. H. Loftus, M. V. Romalis, B. R. Heckel, and E. N. Fortson, "Improved limit on the permanent electric dipole moment of Hg-199," *Physical Review Letters*, vol. 102, no. 10, Article ID 101601, 2009.

[36] S. Abel, S. Khalil, and O. Lebedev, "EDM constraints in supersymmetric theories," *Nuclear Physics B*, vol. 606, no. 1-2, pp. 151–182, 2001.

[37] N. Haba, "Explicit *CP* violation in the Higgs sector of the next-to-minimal supersymmetric standard model," *Progress of Theoretical Physics*, vol. 97, no. 2, pp. 301–309, 1997.

[38] T. Ibrahim and P. Nath, "The neutron and the lepton EDMs in MSSM, large CP violating phases, and the cancellation mechanism," *Physical Review D*, vol. 58, Article ID 111301, 1998.

[39] M. Boz, "The Higgs sector and electron electric dipole moment in next-to-minimal supersymmetry with explicit CP violation," *Modern Physics Letters A*, vol. 21, no. 3, pp. 243–264, 2006.

[40] J. R. Ellis, J. S. Lee, and A. Pilaftsis, "Electric dipole moments in the MSSM reloaded," *Journal of High Energy Physics*, vol. 2008, no. 10, article 049, 2008.

[41] Y. Li, S. Profumo, and M. Ramsey-Musolf, "A comprehensive analysis of electric dipole moment constraints on CP-violating phases in the MSSM," *Journal of High Energy Physics*, vol. 2010, article 62, 2010.

[42] S. J. Huber and M. G. Schmidt, "Electroweak baryogenesis: concrete in a SUSY model with a gauge singlet," *Nuclear Physics B*, vol. 606, no. 1-2, pp. 183–230, 2001.

[43] S. J. Huber, T. Konstandin, T. Prokopec, and M. G. Schmidt, "Baryogenesis in the MSSM, nMSSM and NMSSM," *Nuclear Physics A*, vol. 785, no. 1-2, pp. 206–209, 2007.

[44] S. Kanemura, E. Senaha, and T. Shindou, "First-order electroweak phase transition powered by additional F-term loop effects in an extended supersymmetric Higgs sector," *Physics Letters, Section B: Nuclear, Elementary Particle and High-Energy Physics*, vol. 706, no. 1, pp. 40–45, 2011.

[45] K. Cheung, T.-J. Hou, J. S. Lee, and E. Senaha, "Singlino-driven electroweak baryogenesis in the next-to-MSSM," *Physics Letters B*, vol. 710, no. 1, pp. 188–191, 2012.

[46] W. Huang, Z. Kang, J. Shu, P. Wu, and J. M. Yang, "New insights in the electroweak phase transition in the NMSSM," *Physical Review D*, vol. 91, no. 2, Article ID 025006, 2015.

[47] X.-J. Bi, L. Bian, W. Huang, J. Shu, and P.-F. Yin, "Interpretation of the Galactic Center excess and electroweak phase transition in the NMSSM," *Physical Review D*, vol. 92, no. 2, Article ID 023507, 2015.

[48] S. Moretti, S. Munir, and P. Poulose, "125 GeV Higgs boson signal within the complex NMSSM," *Physical Review D*, vol. 89, Article ID 015022, 2014.

[49] D. A. Demir, "Effects of the supersymmetric phases on the neutral Higgs sector," *Physical Review D*, vol. 60, Article ID 055006, 1999.

[50] A. Dedes and S. Moretti, "Effect of large supersymmetric phases on Higgs production," *Physical Review Letters*, vol. 84, no. 1, pp. 22–25, 2000.

[51] A. Dedes and S. Moretti, "Effects of CP violating phases on Higgs boson production at hadron colliders in the minimal supersymmetric standard model," *Nuclear Physics B*, vol. 576, pp. 29–55, 2000.

[52] G. L. Kane and L.-T. Wang, "Implications of supersymmetry phases for Higgs boson signals and limits," *Physics Letters B*, vol. 488, no. 3-4, pp. 383–389, 2000.

[53] A. Arhrib, D. K. Ghosh, and O. C. W. Kong, "Observing CP violating MSSM Higgs bosons at hadron colliders?" *Physics Letters B*, vol. 537, no. 3-4, pp. 217–226, 2002.

[54] S. Y. Choi, K. Hagivvara, and J. S. Lee, "Higgs boson decays in the minimal supersymmetric standard model with radiative Higgs sector CP violation," *Physical Review D*, vol. 64, no. 3, Article ID 032004, 2001.

[55] S. Y. Choi, M. Drees, J. S. Lee, and J. Song, "Supersymmetric Higgs boson decays in the MSSM with explicit CP violation," *European Physical Journal C*, vol. 25, no. 2, pp. 307–313, 2002.

[56] J. R. Ellis, J. S. Lee, and A. Pilaftsis, "CERN LHC signatures of resonant CP violation in a minimal supersymmetric Higgs sector," *Physical Review D*, vol. 70, Article ID 075010, 2004.

[57] S. Hesselbach, S. Moretti, S. Munir, and P. Poulose, "Explicit CP violation in the MSSM through $gg \to H_1 \to \gamma\gamma$," *Physical Review D*, vol. 82, Article ID 074004, 2010.

[58] T. Fritzsche, S. Heinemeyer, H. Rzehak, and C. Schappacher, "Heavy scalar top quark decays in the complex MSSM: a full one-loop analysis," *Physical Review D*, vol. 86, no. 3, Article ID 035014, 2012.

[59] A. Chakraborty, B. Das, J. L. Diaz-Cruz, D. K. Ghosh, S. Moretti, and P. Poulose, "125 GeV Higgs signal at the LHC in the *CP*-violating MSSM," *Physical Review D*, vol. 90, no. 5, Article ID 055005, 2014.

[60] K. Funakubo, S. Tao, and F. Toyoda, "Phase transitions in the NMSSM," *Progress of Theoretical Physics*, vol. 114, no. 2, pp. 369–389, 2005.

[61] S. W. Ham, S. K. Oh, and D. Son, "Neutral Higgs sector of the next-to-minimal supersymmetric standard model with explicit CP violation," *Physical Review D*, vol. 65, Article ID 075004, 2002.

[62] K. Funakubo and S. Tao, "The Higgs sector in the next-to-MSSM," *Progress of Theoretical Physics*, vol. 113, no. 4, pp. 821–842, 2005.

[63] K. Cheung, T.-J. Hou, J. S. Lee, and E. Senaha, "The Higgs boson sector of the Nextto-MSSM with CP violation," *Physical Review D*, vol. 82, Article ID 075007, 2010.

[64] K. Cheung, T.-J. Hou, J. S. Lee, and E. Senaha, "Higgs-mediated electric-dipole moments in the next-to-minimal supersymmetric standard model: an application to electroweak baryogenesis," *Physical Review D*, vol. 84, Article ID 015002, 2011.

[65] S. Munir, "Novel Higgs-to-125 GeV Higgs boson decays in the complex NMSSM," *Physical Review D*, vol. 89, Article ID 095013, 2014.

[66] F. Domingo, "A new tool for the study of the CP-violating NMSSM," *Journal of High Energy Physics*, vol. 2015, no. 6, article 052, 2015.

[67] T. Graf, R. Gröber, M. Mühlleitner, H. Rzehak, and K. Walz, "Higgs boson masses in the complex NMSSM at one-loop level," *Journal of High Energy Physics*, vol. 2012, no. 10, article 122, 2012.

[68] M. Muhlleitner, D. T. Nhung, H. Rzehak, and K. Walz, "Two-loop contributions of the order $\mathcal{O}(\alpha_t\alpha_s)$ to the masses of the Higgs bosons in the CP-violating NMSSM," *Journal of High Energy Physics*, vol. 2015, article 128, 2015.

[69] V. Khachatryan, A. M. Sirunyan, A. Tumasyan et al., "Precise determination of the mass of the Higgs boson and tests of compatibility of its couplings with the standard model predictions using proton collisions at 7 and 8TeV," *The European Physical Journal C*, vol. 75, no. 5, article 212, 2015.

[70] ATLAS Collaboration, "Updated coupling measurements of the Higgs boson with the ATLAS detector using up to 25 fb^{-1} of proton-proton collision data," Tech. Rep. ATLAS-CONF-2014-009, CERN, Geneva, Switzerland, 2014.

[71] J. Baglio, R. Gröber, M. Mühlleitner et al., "NMSSMCALC: a program package for the calculation of loop-corrected Higgs boson masses and decay widths in the (complex) NMSSM," *Computer Physics Communications*, vol. 185, no. 12, pp. 3372–3391, 2014.

[72] G. Aad, B. Abbott, J. Abdallah et al., "Combined measurement of the boson mass in *pp* collisions at $\sqrt{s} = 7$ and 8 TeV with the ATLAS and CMS experiments," *Physical Review Letters*, vol. 114, Article ID 191803, 2015.

[73] P. Bechtle, S. Heinemeyer, O. Stål, T. Stefaniak, and G. Weiglein, "HiggsSignals: confronting arbitrary Higgs sectors with measurements at the Tevatron and the LHC," *The European Physical Journal C*, vol. 74, no. 2, article 2711, 2014.

[74] J. F. Gunion, Y. Jiang, and S. Kraml, "Diagnosing degenerate Higgs bosons at 125 GeV," *Physical Review Letters*, vol. 110, no. 5, Article ID 051801, 2013.

[75] M. D. Goodsell, K. Nickel, and F. Staub, "Two-loop corrections to the Higgs masses in the NMSSM," *Physical Review D*, vol. 91, no. 3, Article ID 035021, 2015.

[76] F. Staub, Privatecommunication.

[77] F. Feroz and M. P. Hobson, "Multimodal nested sampling: an efficient and robust alternative to Markov Chain Monte Carlo methods for astronomical data analyses," *Monthly Notices of the Royal Astronomical Society*, vol. 384, no. 2, pp. 449–463, 2008.

[78] F. Feroz, M. P. Hobson, and M. Bridges, "MultiNest: an efficient and robust Bayesian inference tool for cosmology and particle physics," *Monthly Notices of the Royal Astronomical Society*, vol. 398, no. 4, pp. 1601–1614, 2009.

[79] F. Feroz, M. P. Hobson, E. Cameron, and A. N. Pettitt, "Importance nested sampling and the MultiNest algorithm," http://arxiv.org/abs/1306.2144.

[80] P. Bechtle, O. Brein, S. Heinemeyer, G. Weiglein, and K. E. Williams, "HiggsBounds: confronting arbitrary Higgs sectors with exclusion bounds from LEP and the Tevatron," *Computer Physics Communications*, vol. 181, no. 1, pp. 138–167, 2010.

[81] P. Bechtle, O. Brein, S. Heinemeyer, G. Weiglein, and K. E. Williams, "HiggsBounds 2.0.0: confronting neutral and charged Higgs sector predictions with exclusion bounds from LEP and the Tevatron," *Computer Physics Communications*, vol. 182, no. 12, pp. 2605–2631, 2011.

[82] P. Bechtle, O. Brein, S. Heinemeyer et al., "Recent Developments in HiggsBounds and a Preview of HiggsSignals," PoS CHARGED2012 (2012) 024, http://xxx.lanl.gov/abs/1301.2345.

[83] P. Bechtle, O. Brein, S. Heinemeyer et al., "HiggsBounds-4 : improved tests of extended Higgs sectors against exclusion bounds from LEP, the Tevatron and the LHC," *The European Physical Journal C*, vol. 74, article 2693, 2014.

[84] A. Djouadi, J. Kalinowski, and M. Spira, "HDECAY: a program for Higgs boson decays in the standard model and its supersymmetric extension," *Computer Physics Communications*, vol. 108, no. 1, pp. 56–74, 1998.

[85] B. Das, S. Moretti, S. Munir, and P. Poulose, In preparation.